Tetrahedron 65 (2009) 9876–9883

Contents lists available at ScienceDirect

Tetrahedron

journal homepage: www.elsevier.com/locate/tet

Phosphorus-supported multidentate coumarin-containing fluorescence sensors for Cu^{2+}

Vadapalli Chandrasekhar*, Prasenjit Bag, Mrituanjay D. Pandey

Department of Chemistry, Indian Institute of Technology Kanpur, Kanpur 208016, India

ARTICLE INFO

Article history:
Received 5 August 2009
Received in revised form
9 September 2009
Accepted 9 September 2009
Available online 23 September 2009

Keywords:
Phosphorus
Coumarin
Fluorescence
C=N bond isomerization
X-ray crystallography

ABSTRACT

Phosphorus hydrazides $PhP(O)[N(Me)NH_2]_2$, $(S)P[N(Me)NH_2]_3$, and $N_3P_3[N(Me)NH_2]_6$ were condensed with 7-diethylaminocoumarin-3-aldehyde (RCHO) to afford the corresponding hydrazones $PhP(O)[N(Me)N{=}CHR]_2$ (**1**), $(S)P[N(Me)N{=}CHR]_3$ (**2**), and $N_3P_3[N(Me)N{=}CHR]_6$ (**3**). The structural characterization of **1**–**3** was carried out by their HRMS, ^1H and $^{31}P\{^1H\}$ NMR spectra. The molecular structure of **2** was established by a single-crystal X-ray analysis. Interaction of **1** and **2** with various transition metal ions revealed substantial fluorescence enhancement upon interaction with Cu^{2+} enabling a selective detection mechanism for this metal ion. However, such a fluorescence enhancement was not observed in the case of **3**. A 1:1 complex $[\mathbf{2}\cdot Zn][ClO_4]_2\cdot 4CH_2Cl_2$ was isolated in the reaction of **2** with $Zn(ClO_4)_2\cdot 6H_2O$. The molecular structure of this complex revealed that the Zn^{II} is encapsulated by the ligand utilizing a 3N, 3O coordination set.

1. Introduction

There is a growing interest in the development of molecular sensors that can detect selectively metal ions even in low concentrations. Among the various techniques used for this purpose fluorescence-based methods[1–9] have gained in importance because of their sensitivity. These methods depend upon the change of fluorescence intensity and/or a shift in the fluorescence band of the sensor upon interaction with the metal ion. Although such a methodology has been successful for diamagnetic metal ions, its application to paramagnetic metal ions is fraught with difficulties in view of the fact that the latter quench fluorescence either via energy or electron transfer[10–12] and only in some instances a fluorescence enhancement has been observed.[13–24] In this regard, development of fluorescence-based sensors for Cu(II)[15–29] has assumed importance in view of the fact that it is an essential trace element and yet at slightly increased concentrations, it is toxic, being implicated in gastrointestinal[30,31], liver, and kidney diseases as well as in neurological diseases such as Alzheimer's[32] or Parkinson's.[33]

Our interest in phosphorus-supported ligands[34,35] has suggested to us the possibility of using phosphorus as a support to build a coordination platform embedded with fluorophores. As a test of this principle we have recently demonstrated the efficiency of this methodology by using pyrene-containing ligands.[36] The widespread use of coumarin-based fluorophores in literature[37–41] has prompted us to prepare phosphorus-supported coumarin-containing ligands and examine them as a selective sensor for Cu^{2+}.

2. Results and discussion

The reaction of phosphorus hydrazides $PhP(O)[N(Me)NH_2]_2$, $(S)P[N(Me)NH_2]_3$, and $N_3P_3[N(Me)NH_2]_6$ with 7-diethylaminocoumarin-3-aldehyde afforded the coumarin-containing ligands **1**–**3** (Chart 1) . The modular nature of the ligand design allowed the variation of the number of fluorophores from two (compound **1**) through three (compound **2**) to six (compound **3**). A representative synthetic protocol is shown in Scheme 1. All these ligands have been characterized by ^1H NMR, ^{31}P NMR, and ESI-HRMS analysis. The molecular structure of **2** was determined by single-crystal X-ray crystallography (Fig. 1a). Although we were unable to obtain crystals for copper complexes we were able to obtain the molecular structure of the Zn^{2+} complex, $[\mathbf{2}\cdot Zn][ClO_4]_2\cdot 4CH_2Cl_2$ (**4**) (Fig. 1b). Selected internuclear distances and bond angles are included in figure captions. Crystal and cell parameter data for **2** and **4** are given in Table 1. Compounds **2** and **4** crystallize in the monoclinic space group $P2_1/n$ (No. 14) and $P2_1/c$ (No. 14), respectively. The molecular structures of both the compounds reveal a central tetrahedral phosphorus atom, which acts as a support to hold the multi-site coordination platform built around it. The P–S bond distances

---

* Corresponding author. Tel.: +91 512 259 7259; fax: +91 512 259 7436.
E-mail address: vc@iitk.ac.in (V. Chandrasekhar).

doi:10.1016/j.tet.2009.09.040

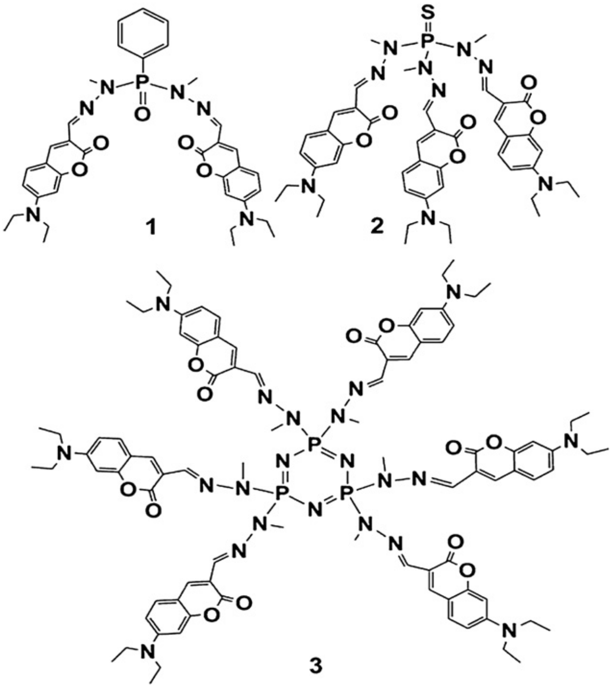

Chart 1. Line-diagrams of **1**, **2**, and **3**.

observed in **2** and **4** are 1.9186(14) Å and 1.9147(31) Å, respectively, which is consistent with P=S distances found in literature.[42] The P–N bond distances in **2** and **4** are 1.6801(31) Å, and 1.6848(69) Å, respectively. This may be compared with the normal P–N single bond distance (observed in P(V) compounds), which is 1.70 Å.[43] Compound **4** shows that Zn(II) is encapsulated by **2** in a 3N, 3O facial coordination environment (Fig. 2). The crystal packing of **2** appears to be effected by the molecular association through C–H···O hydrogen bonds (Fig. 3) and **4** shows that it forms a one-dimensional chain via perchlorate ions as a result of CH···O interactions (Fig. 4) and via π–π stacking (Fig. 5). Hydrogen bond parameters for these compounds are given in Table 2.

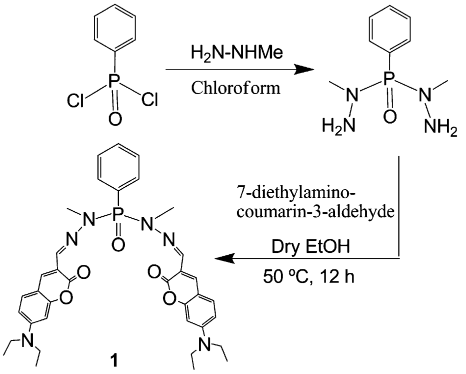

Scheme 1. Synthesis of **1**.

The absorption spectra of **1**–**3** in acetonitrile are characterized by peaks both at high and low energies (Table 3). Although $\lambda_{\max}$ (Fig. 6a) remains invariant [cf. **1**, $\lambda_{\max}$ (ϵ); 270 (30,000), 316 (9634), 424 (71,500); **2**, 271 (4.99×10^4), 316 (9.97×10^3), 413 (9.17×10^4); **3**, 270 (5.03×10^4), 317 (1.32×10^4), 423 (1.06×10^5)] absorbance value increases as the number of coumarin arms increase from two (**1**) to six (**3**). Compounds **1**–**3** show an emission around 500 nm upon excitation at 413 nm. The fluorescence intensity remains almost the same and is of low intensity in all these three ligands (Fig. 6b).

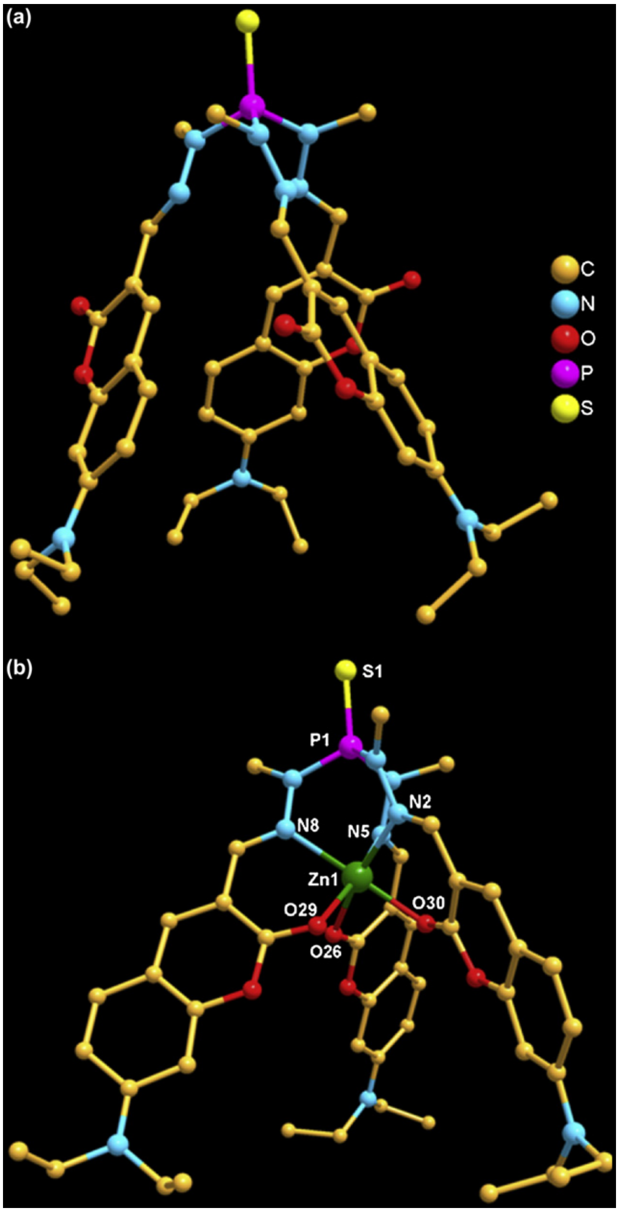

Figure 1. Molecular structure of (a) **2**, (b) **4** (solvent molecules and hydrogen atoms have been omitted for clarity). Selected bond distances (Å) and angles (°) are as follows: **2**: N(1)–P(1), 1.666(3); N(4)–P(1), 1.677(3); N(7)–P(1), 1.665(3); N(10)–P(2), 1.670(3); N(13)–P(2), 1.670(3); N(16)–P(2), 1.680(3); P(1)–S(1), 1.9194(13); P(2)S(2), 1.9187(13); N(5)–N(4)–P(1), 113.4(2); C(17)–N(4)–P(1), 119.8(2); N(8)–N(7)–P(1), 113.4(2); C(32)–N(7)–P(1), 122.9(2); N(11)–N(10)–P(2), 114.4(2); C(47)–N(10)–P(2), 119.5(2); N(14)–N(13)–P(2), 113.6(2); C(62)–N(13)–P(2), 121.6(2); N(17)–N(16)–P(2), 112.7(2); C(77)–N(16)–P(2), 121.4(2); N(7)–P(1)–N(1), 104.44(15); N(7)–P(1)–N(4), 106.18(15); N(1)–P(1)–N(4), 105.33(15); N(7)–P(1)–S(1), 113.59(12); N(1)–P(1)–S(1), 113.32(11); N(4)–P(1)–S(1), 113.17(11); N(13)–P(2)–N(10), 104.39(15); N(13)–P(2)–N(16), 106.08(15); N(10)–P(2)–N(16), 105.73(15); N(13)–P(2)–S(2), 112.82(12); N(10)–P(2)–S(2), 113.07(11); N(16)–P(2)–S(2), 113.97(12). **4**: N(1)–P(1), 1.685(6); N(4)–P(1), 1.690(7); N(7)–P(1), 1.653(7); P(1)–S(1), 1.915(3); N(2)–N(1)–P(1), 115.1(5); C(1)–N(1)–P(1), 123.8(5); N(5)–N(4)–P(1), 114.8(5); C(16)–N(4)–P(1), 119.3(6); N(8)–N(7)–P(1), 118.0(5); C(31)–N(7)–P(1), 121.7(6); N(7)–P(1)–N(1), 106.7(3); N(7)–P(1)–N(4), 104.7(3); N(1)–P(1)–N(4), 105.1(3); N(7)–P(1)–S(1), 113.4(3); N(1)–P(1)–S(1), 113.0(3); N(4)–P(1)–S(1), 113.1(3).

Interaction of **1** or **2** with various metal ions (Fig. 7) showed that only with Cu(II) the titration curves revealed isosbestic point at 285 and 360 nm indicating the formation of a 1:1 complex (Fig. 8). This conclusion is also supported by ESI-MS analysis of the isolated complexes. Three major peaks at *m*/*z* 365.24 [**1**+Cu]$^{2+}$, 471.14 [**2**+Cu]$^{2+}$, and 915.83 [**3**+Cu]$^{2+}$ are seen. Although single crystals of

Table 1
Crystallographic data and structure refinement details for **2** and **4**

	2	**4**
Identification code	3junbm	22maybm
Empirical formula	$C_{23.50}H_{27}N_5O_3P_{0.50}S_{0.50}$	$C_{49}H_{62}C_{l10}N_9O_{14}PSZn$
Formula weight	459.02	1483.98
Temperature (K)	100(2) K	100(2) K
Wavelength (Å)	0.71073 Å	0.71073 Å
Crystal system	Monoclinic	Monoclinic
Space group	$P2_1/n$	$P2_1/c$
Unit cell dimensions (Å), (°)	a=16.330(3) Å α=90°	a=13.424(3) Å α=90°
	b=19.742(4) Å β=95.117(4)°	b=22.161(5) Å β=91.655(4)°
	c=30.383(6) Å γ=90°	c=21.299(4) Å γ=90°
Volume (Å^3)	9756(3) Å^3	6334(2) Å^3
Z	16	4
Density (calculated) (Mg/m^3)	1.250 Mg/m^3	1.556 Mg/m^3
Absorption coefficient (mm^{-1})	0.156 mm^{-1}	0.936 mm^{-1}
F(000)	3880	3048
Crystal size (mm^3)	0.103×0.082×0.056 mm^3	0.088×0.054×0.031 mm^3
Theta range for data collection (°)	2.04–28.37°	2.04–26.00°
Index ranges	$-21 \le h \le 21$, $-20 \le k \le 26$, $-40 \le l \le 40$	$-16 \le h \le 15$, $-27 \le k \le 27$, $-26 \le l \le 20$
Reflections collected	63,762	34,768
Independent reflections	23,997 [R(int)=0.0995]	12,417 [R(int)=0.1013]
Completeness to theta	98.2% (28.37°)	99.8% (26.00°)
Absorption correction	None	None
Max. and min. transmission		
Refinement method	Full-matrix least-squares on F^2	Full-matrix least-squares on F^2
Data/restraints/parameters	23,997/0/1200	12,417/0/775
Goodness-of-fit on F^2	1.018	1.055
Final R indices [$I>2\sigma(I)$]	$R1$=0.0819, $wR2$=0.2000	$R1$=0.0878, $wR2$=0.2402
R indices (all data)	$R1$=0.1710, $wR2$=0.2642	$R1$=0.1602, $wR2$=0.2749
Largest diff. peak and hole (e Å^{-3})	1.627 and −0.585 e Å^{-3}	1.097 and −0.758 e Å^{-3}

the copper complexes could not be isolated the coordination mode of **2** is revealed in its interaction with Zn(II) (vide supra).

Interestingly, among the various metal ions that were tried, only Cu^{2+} influences the fluorescence of **1** and **2** (Fig. 9). First, a blue shift in emission maxima is observed (495–480 nm in the case of **1**; 500–481 nm in the case of **2**). Secondly the fluorescence intensity of the free ligands increases abruptly upon addition of the metal ion (Fig. 10). The fluorescence enhancement factors (FEFs) in terms of quantum yield for **1** and **2** upon binding with Cu^{2+} are 15 and 10, respectively. In contrast, the hexa-armed ligand **3** does not show any appreciable increase of its intensity upon interaction with Cu^{2+}. The FEFs found for **1** and **2** seem to be a reflection of their efficiency to bind Cu^{2+}. Thus, the binding constants[44,45] of **1** and **2** with respect to Cu^{2+} are quite high: $K_s=1.9\times10^5$ and 6.1×10^4, respectively, in comparison with other metal ions. Additionally, the binding of Cu^{2+} with **1** or **2**, and the consequent FEFs are not affected in the presence of other metal ions (Fig. 11).

The fluorescence enhancement observed in the present instance appears to be result of the prevention of C=N bond isomerization.[39,40] In the free ligands C=N isomerization is facile as a result of free rotation around this bond in the excited state. However metal ion binding locks this bond and free rotation is prevented. Additionally, in the free ligand, photoinduced electron transfer of the lone pair of electrons on nitrogen would be quenching the fluorescence. Metalation with Cu^{2+} thwarts both of these non-emissive pathways, leading to a revival of fluorescence (Scheme 2). In the case of **3**, presumably, steric hindrance prevents complete involvement of all the coordinating arms in metal ion binding. Thus, even if two arms are involved in binding four others are not. As a result, fluorescence enhancement is minimal.

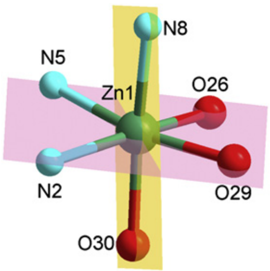

Figure 2. Coordination environment around zinc. Selected bond distances (Å) and angles (°) are as follows: O(29)–Zn(1)–O(30), 86.1(2); N(2)–Zn(1), 2.156(7); O(29)–Zn(1)–N(5), 167.8(2); N(5)–Zn(1), 2.102(6); O(30)–Zn(1)–N(5), 101.4(2); N(8)–Zn(1), 2.106(6); O(29)–Zn(1)–O(26), 86.4(2); O(26)–Zn(1), 2.105(5); O(30)–Zn(1)–O(26), 88.7(2); O(29)–Zn(1), 2.052(5); N(5)–Zn(1)–O(26), 84.2(2); O(30)–Zn(1), 2.053(5); O(29)–Zn(1)–N(8), 85.1(2); O(30)–Zn(1)–N(8), 167.9(2); N(5)–Zn(1)–N(8), 88.7(2); O(26)–Zn(1)–N(8), 99.1(2); O(29)–Zn(1)–N(2), 101.6(2); O(30)–Zn(1)–N(2), 85.0(2); N(5)–Zn(1)–N(2), 88.7(2); O(26)–Zn(1)–N(2), 169.4(2); N(8)–Zn(1)–N(2), 88.6(3); O(29)–Zn(1)–O(30), 86.1(2); O(29)–Zn(1)–N(5), 167.8(2); O(30)–Zn(1)–N(5), 101.4(2).

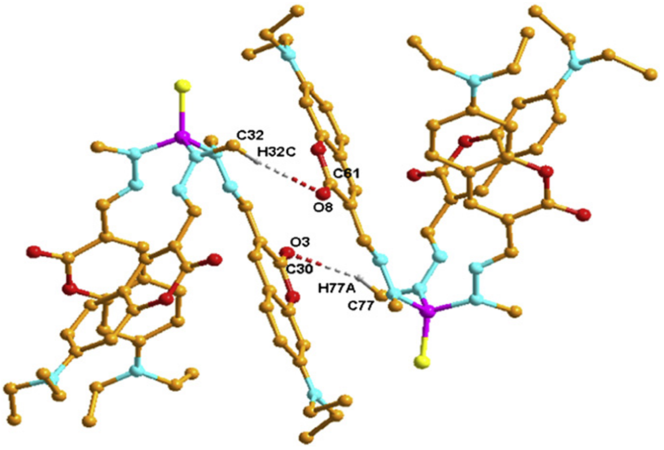

Figure 3. Formation of chain in **2** via intermolecular hydrogen bonding. Color code: orange, carbon; turquoise, nitrogen; red, oxygen; pink, phosphorus; yellow, sulfur.

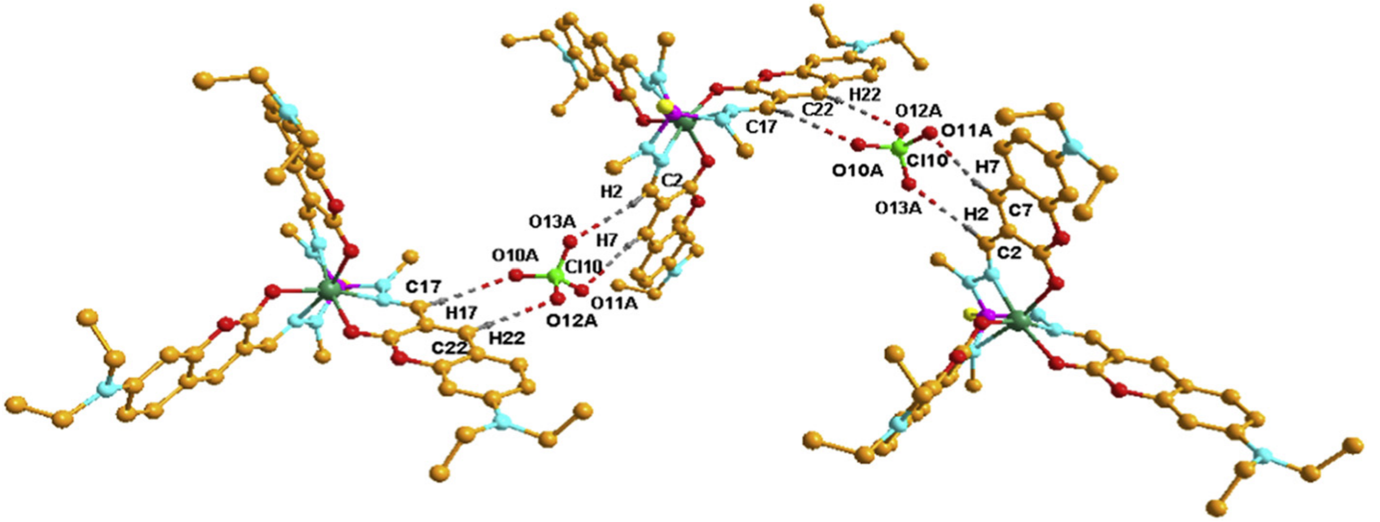

Figure 4. Formation of chain in **4** via intermolecular hydrogen bonding.

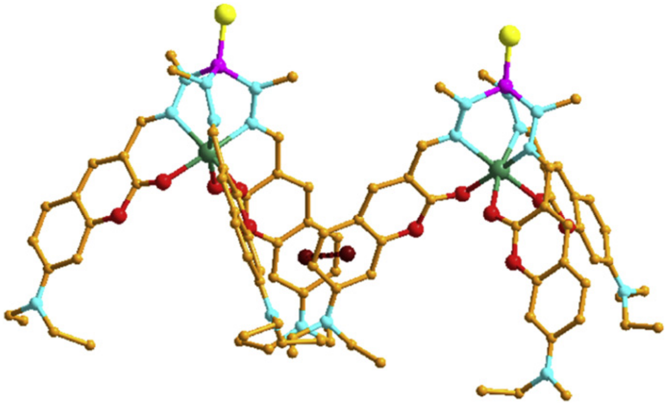

Figure 5. Interplay of intramolecular π–π interaction showing supramolecular architecture. Bond length is 3.7776(6) Å and symmetry (*x*,*y*,*z*).

3. Experimental

3.1. General experimental information

Fluorescence spectra were recorded on a Varian Luminescence Cary eclipsed and electronic spectra were recorded on a Perkin–Elmer-Lambda 20 UV–vis spectrometer with a 10 mm quartz cell at 25±0.1 °C. Melting points were measured using a JSGW melting point apparatus and are uncorrected. ^{1}H NMR spectra were obtained on a JEOL-JNM LAMBDA 400 model spectrometer operating at 400.0 MHz. ^{1}H and ^{31}P NMR spectra were also obtained on a JEOL-DELTA2 500 model spectrometer operating at 500 and 202.5 MHz, respectively. The chemical shifts are referenced with respect to TMS for ^{1}H and 85% H_3PO_4 for ^{31}P. Electrospray ionization-high resolution mass spectra (ESI-HRMS) were recorded on a MICROMASS QUATTRO II triple quadrupole mass spectrometer. The ESI capillary was set at 3.5 kV and the cone voltage was 40 V. The crystal data for compounds **1**, **2**, and **3** were collected on a Bruker SMART APEX CCD Diffractometer. The program SMART (version 6.45) was used for integration of the intensity of reflections and scaling. The program SADABS was used for absorption correction. The crystal structures were solved and refined by full-matrix least-squares methods against F^2 by using the program SHELXTL-97.[46] All non-hydrogen atoms were refined with anisotropic displacement parameters. Hydrogen positions were fixed at calculated positions and refined isotropically. The figures are generated by using Diamond 3.1e programme. Crystal data for compounds **2** and **4** are given in Table 1. Ph_2POCl, $PhPOCl_2$, $N_3P_3Cl_6$ and metal salts $Cu(ClO_4)_2\cdot 6H_2O$, $LiClO_4$, and $NaClO_4\cdot H_2O$ were purchased from Aldrich. $Co(ClO_4)_2\cdot 6H_2O$, $Zn(ClO_4)_2\cdot 6H_2O$, $Cd(ClO_4)_2\cdot 6H_2O$, $Ni(ClO_4)_2\cdot 6H_2O$, $Mg(ClO_4)_2\cdot 6H_2O$, and $Ca(ClO_4)_2\cdot 4H_2O$ were prepared from their carbonate salts by a reaction with perchloric acid. (*S*)PCl_3 was purchased from Fluka (Switzerland). 7-Diethylaminocoumarin-3-aldehyde synthesized by reported method.[39,40] *N*-Methylhydrazine was obtained as a gift from the Vikram Sarabhai Space Research Centre, Thiruvananthapuram, India. Solvents were purchased from S.D. Fine Chemicals (India) and they were purified prior to use.

Fluorescence quantum yields in each case were determined by comparing the emission intensity of the sample with that of the fluorescence standard, fluorescein[47,48] ($\Phi = 0.85$) in 0.1 N NaOH using the following equation:

$$\Phi_U = \Phi_R(A_U/A_R)\left(n_U^2/n_R^2\right)$$

where A_U and A_R are the integrated area under the corrected fluorescence spectra for the sample and reference, n_U and n_R are the refractive indices of the sample and reference, respectively.

Table 2
Hydrogen bond parameters

Compounds	D–H···A	*d*(D–H)	*d*(H···A)	*d*(D···A)	∠(DHA)	Symmetry
4	C32–H32C···O8	0.93	2.4388(17)	3.4423(45)	173.041 (228)	(−1+*x*, −1+*y*, −1+*z*)
	C77–H77A···O3	0.93	2.5093(26)	3.4415(45)	158.651 (228)	(0.5−*x*, −0.5+*y*, 0.5−*z*)
	C17–H17···O10A	0.93	2.6476(66)	3.4591(109)	146.262 (554)	(1−*x*, −0.5+*y*, 0.5−*z*)
	C22–H22A···O12A	0.93	2.4471(76)	3.2483(105)	144.425 (471)	(1−*x*, −0.5+*y*, 0.5−*z*)
2	C7–H7···O11A	0.93	2.4564(66)	3.3457(102)	159.497 (492)	(1−*x*, −0.5+*y*, 0.5−*z*)
	C2–H2A···O13A	0.93	2.5624(66)	3.414(10)	152.513 (480)	(1−*x*, −0.5+*y*, 0.5−*z*)

Table 3
Photophysical data of **1** with and without the presence of metal ions[a,b]

Compound	λ_{max}, nm (ε)	λ_{em}, nm	Φ_F	K_a, M^{-1}
1	270 (30,000), 316 (9.97×10^3), 425 (7.147×10^4)	495	0.0185	—
2	271 (4.99×10^4), 316 (9.97×10^3), 413 (9.17×10^4)	500	0.0155	—
3	270 (5.03×10^4), 317 (1.32×10^4), 423 (1.06×10^5)	504	0.0146	—
1+Cu	271 (2.18×10^4), 310 (1.77×10^4), 443 (5.31×10^4)	480	0.2848	1.9×10^5
2+Cu	270 (3.43×10^4), 315 (3.12×10^4), 438 (1.13×10^5)	481	0.1545	6.1×10^4
3+Cu	270 (7.65×10^4), 316 (3.64×10^4), 427 (1.64×10^5)	48	0.0175	1.8×10^4
1+Mg	274 (2.46×10^4), 305 (2.2×10^4), 458 (9.55×10^4)	497	—	2.4×10^4
2+Mg	305 (4.01×10^4), 430 (1.44×10^5), 476 (1.548×10^5)	508	—	5.6×10^4
1+Zn	274 (2.11×10^4), 303 (2.23×10^4), 453 (9.34×10^4)	498	—	1.5×10^4
2+Zn	266, 305 (4.12×10^4), 430 (1.62×10^5), 479 (1.61×10^5)	508	—	1.7×10^4

[a] Metal salt used: $Cu(ClO_4)_2\cdot6H_2O$, $Zn(ClO_4)_2\cdot6H_2O$ and $Mg(ClO_4)_2\cdot6H_2O$.

[b] Concentration of each metal ion used: 10 µM.

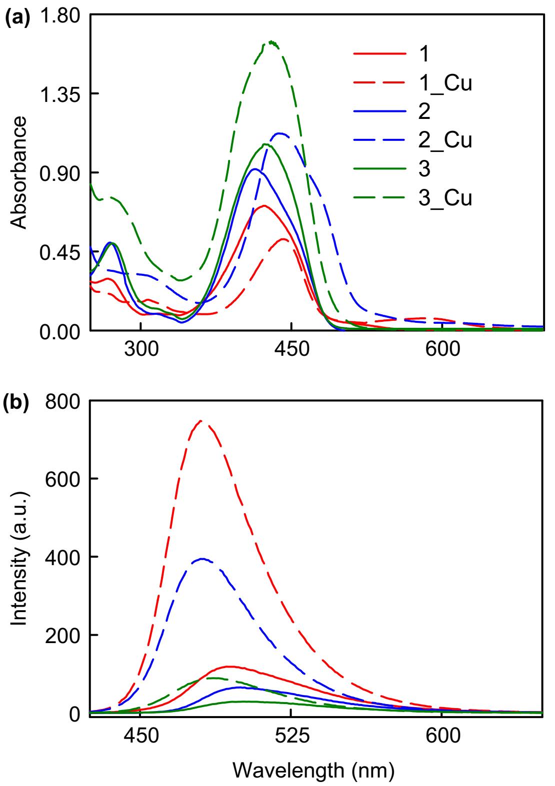

Figure 6. (a) UV–vis spectra of **1**, **2**, and **3** (10 µM) and upon addition of 10 equiv of $Cu(ClO_4)_2\cdot6H_2O$ in CH_3CN. (b) Fluorescence spectra of **1**, **2**, and **3** (10 µM) and upon addition of 10 equiv of $Cu(ClO_4)_2\cdot6H_2O$ in CH_3CN. The excitation wavelength was 413 nm.

The stability constant K_s was determined[49,50] from the fluorescence titration data of the ligand solutions (10^{-5} M) against different metal ion concentration using the following equation.

$$I_F^0/\left(I_F - I_F^0\right) = [a/(b-a)][(1/K_s[M])+1]$$

Where I_F^0 and I_F are the fluorescence intensity of the metal-free ligand and the ML complex, respectively; [M] is the concentration of the metal ions added for complexation. K_s is obtained as intercept/slope ratio from the plot of $I_F^0/(I_F-I_F^0)$ against $[M]^{-1}$.

3.2. General procedure for the synthesis of 1, 2, and 3

7-Diethylaminocoumarin-3-aldehyde was dissolved in hot absolute ethanol (30 ml) and to it an ethanolic solution of the corresponding hydrazide[34,51] was added dropwise for 10 min. The resulting solution was stirred at 50 °C for 12 h. A precipitate was obtained, which was filtered and washed with ethanol three times, followed by recrystallization from CH_2Cl_2/*n*-hexane mixture at 0 °C.

*3.2.1. Compound **1***. $PhPO[(N(CH_3)NH_2]_2$ (0.08 g, 0.167 mmol); 7-diethylaminocoumarin-3-aldehyde (0.20 g, 3.34 mmol); **1** (0.21 g, 0.32 mmol) in 80.0% yield. Mp 195 °C. FTIR (KBr) (ν/cm^{-1}): 3500m, 2924s, 1711s, 1600s, 1516s, 1352s, 1128s, 957s. ^{1}H NMR ($CDCl_3$, 400 MHz): 3.14 (d, 18H, $-NCH_3$); ^3J (^{1}H–^{31}P)=12.0 Hz), 8.74 (s, 2H, imino), 7.87–6.39 (m, 13H, aromatic), 3.34 (m, 8H), 1.12 (t, 12H). ^{13}C NMR (500 MHz, $CDCl_3$, 25 °C, TMS) δ (ppm)=12.53, 31.46, 44.97, 97.25, 108.91, 109.40, 115.25, 128.01, 128.12, 129.89, 131.87, 133.20, 133.27, 137.05, 150.84, 156.37, 162.39. ^{31}P NMR ($CDCl_3$, 500 MHz): 25.65 (s). Anal. Calcd for $C_{36}H_{41}N_6O_5P$; ESI-HRMS: *m*/*z* (%): $[M+H]^+$=calculated 669.2954, found 669.2952.

*3.2.2. Compound **2***. $P(S)[N(CH_3)NH_2]_3$ (0.16 g, 0.81 mmol); 7-diethylaminocoumarin-3-aldehyde (0.60 g, 2.44 mmol); **2** (0.60 g, 0.69 mmol) in 72.90% yield. Mp 230 °C (d). Crystals suitable for single-crystal X-ray diffraction were obtained after dissolving the compound in hot acetonitrile and keeping it at room temperature for 1 day. FTIR (KBr) (ν/cm^{-1}): 3448m, 2970s, 1711s, 1599s, 1518s, 1411s, 1354s, 1257s,

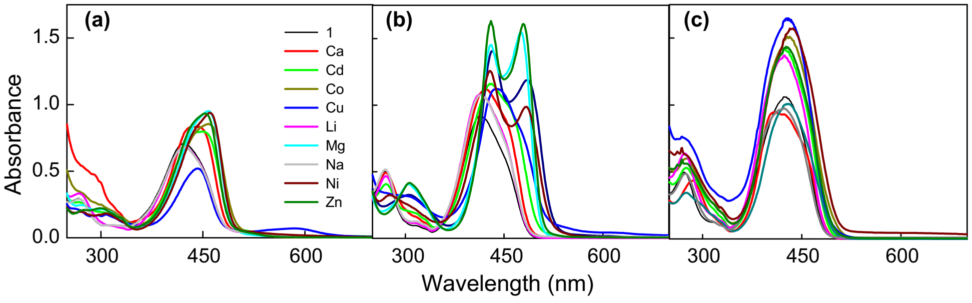

Figure 7. Optical absorption spectra of free ligands, **1** (a), **2** (b), and **3** (c) (10 µM) along with different metal ions (100 µM) in acetonitrile.

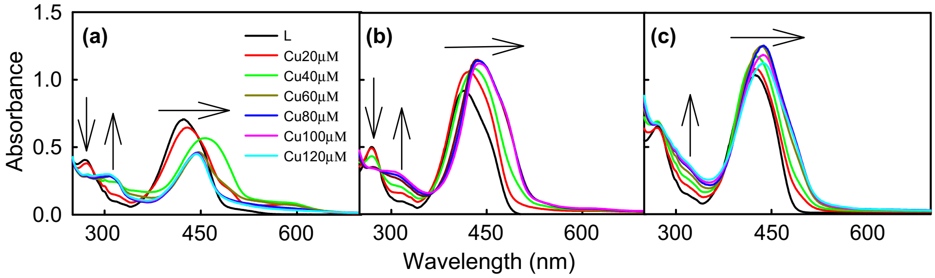

Figure 8. Absorption spectra of **1** (a), **2** (b), and **3** (c) (10 μM) in acetonitrile upon addition of increasing concentrations of $Cu(ClO_4)_2\cdot6H_2O$ (0, 20, 40, 60, 80, 100, and 120 μM).

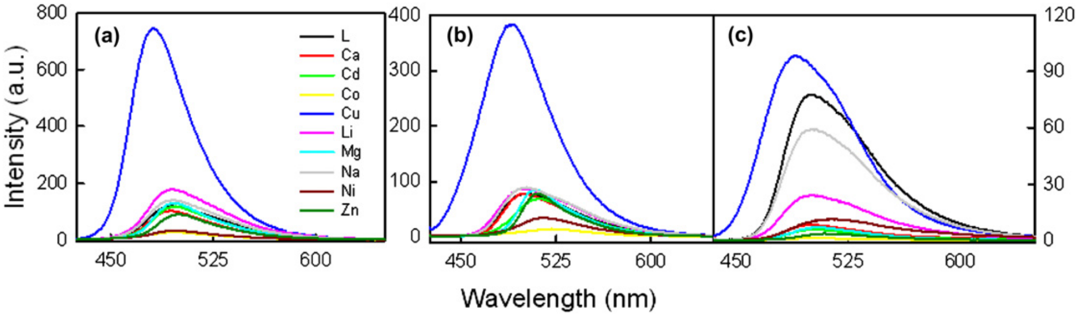

Figure 9. Emission spectra of **1** (a), **2** (b), and **3** (c) (10 μM) and upon addition of 10 equiv of various metal perchlorate salts in acetonitrile solution. The excitation wavelength was 413 nm.

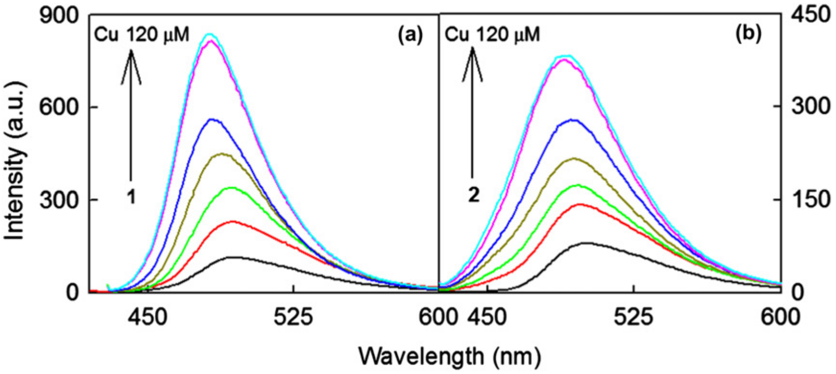

Figure 10. Fluorescence spectra of **1** (a) and **2** (b) (10 μM) in CH_3CN upon addition of increasing concentrations of $Cu(ClO_4)_2\cdot6H_2O$ (0, 20, 40, 60, 80, 100, and 120 μM) with an excitation wavelength of 413 nm.

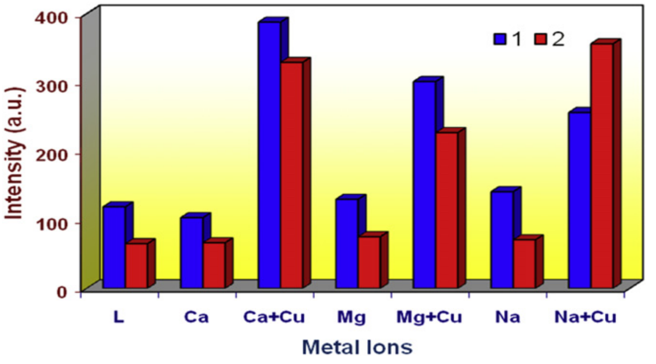

Figure 11. Emission response of **1** or **2** in the presence of various metal ions and a mixture of metal ions. The concentration of $Cu(ClO_4)_2\cdot6H_2O$ was 5 μM while the other metal perchlorates [$Ca(ClO_4)_2\cdot4H_2O$, $Na(ClO_4)_2\cdot H_2O$, and $Mg(ClO_4)_2\cdot6H_2O$] was 10 μM.

1132s, 954s. ^1H NMR ($CDCl_3$, 400 MHz): 3.24 (d, 9H, $-NCH_3$); ^3J ($^1H-^{31}P$)=12.0 Hz, 7.84 (s, 3H, imino), 7.75 (s, 3H), 7.15 (d, 3H), 6.41 (d, 3H), 6.35 (s, 3H), 3.31 (q, 12H), 1.11 (t, 18H). ^{13}C NMR (500 MHz, $CDCl_3$, 25 °C, TMS) δ (ppm)=12.51, 32.82, 44.93, 96.99, 108.97, 109.59, 115.08, 130.08, 131.67, 131.80, 137.12, 150.80, 156.32, 162.58. ^{31}P NMR ($CDCl_3$, 500 MHz): 74.28 (s). Anal. Calcd for $C_{45}H_{54}N_9O_6PS$; ESI-HRMS: m/z (%): $[M+H]^+$=calculated 880.3734, found 880.3674.

3.2.3. Compound ***3***. $N_3P_3[(NCH_3)NH_2]_6$ (0.22 g, 0.55 mmol); 7-diethylaminocoumarin-3-aldehyde (0.82 g, 3.34 mmol); **3** (0.70 g, 0.95 mmol) in 70.94% yield. Mp 220 °C(d). FTIR (KBr) (ν/cm^{-1}): 3452m, 2925s, 1710s, 1598s, 1518s, 1409s, 1305s, 1132s, 967s. ^1H NMR ($CDCl_3$, 400 MHz): 3.27 (d, 18H, $-NCH_3$); ^3J ($^1H-^{31}P$)=12.0 Hz, 8.04 (s, 6H, imino), 7.69 (s, 6H), 7.19 (d, 6H), 6.47 (d, 6H), 6.38 (s, 6H), 3.33 (q, 24), 1.12 (t, 36H). ^{13}C NMR (500 MHz, $CDCl_3$, 25 °C, TMS) δ (ppm)=12.56, 32.56, 44.93, 97.14, 109.09, 109.47, 115.64, 129.96, 136.95, 150.63, 156.24, 162.58. ^{31}P

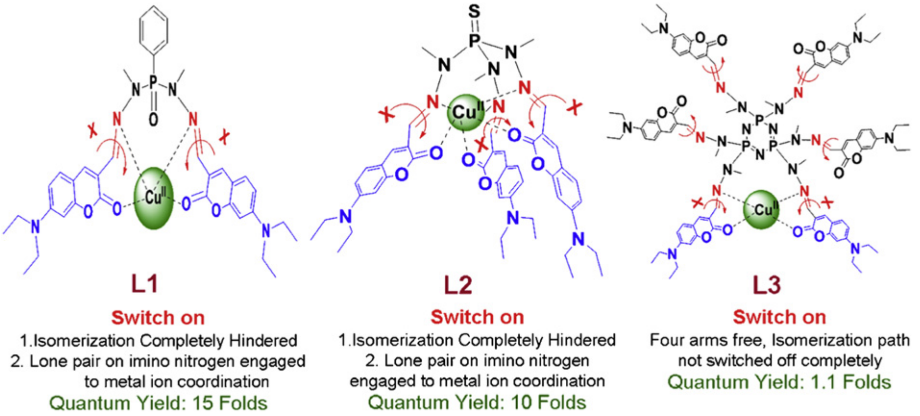

Scheme 2. Schematic representation of the probable mechanism involved in the fluorescence enhancement after metalation.

NMR ($CDCl_3$, 500 MHz): 19.62 (s). Anal. Calcd for $C_{90}H_{108}N_{21}O_{12}P_3$; ESI-HRMS: *m*/*z* (%): $[M+H]^+$=calculated 1769.7811, found 1769.7593.

3.3. General procedure for synthesis of metal complexes

Metal perchlorate salts were dissolved in 30 ml of dry MeOH and were added to a solution of the ligand in dry CH_2Cl_2 (30 ml). The stoichiometry of the reaction was kept at 1:1. The solution was allowed to stir for 12 h at room temperature and then filtered. The filtrate was then evaporated to dryness in vacuum to afford the metal complexes. Only four complexes were isolated and characterized by ESI-MS studies. One of them, compound **4**, the Zn(II) complex formed with ligand **2** was also characterized by single-crystal X-ray diffraction.

3.3.1. Synthesis of the complex ***4***. $Zn(ClO_4)_2\cdot 6H_2O$ (0.38 g, 0.09 mmol); **2** (0.80 g, 0.09 mmol). Orange-red complex was dissolved in ∼5 ml of CH_2Cl_2 and *n*-hexane was added to it until a slight turbidity appeared and kept at 5 °C to obtain a crystalline product. Yield: 0.08 g, 78.86%. FTIR (KBr) (ν/cm^{-1}): 3449b, 2973m, 2930m, 1707s, 1657s, 1572s, 1512s, 1424m, 1350s, 1259m, 1133s, 956s. ^{1}H NMR ($CDCl_3$, 400 MHz): 3.27 (d, 9H, $-NCH_3$); ^3J ($^1H-^{31}P$)=12.0 Hz, 8.26 (s, 3H, imino), 7.75 (s, 3H), 7.17 (d, 3H), 6.43 (d, 3H), 6.35 (s, 3H), 3.37 (q, 12H), 1.18 (t, 18H). ESI-HRMS: *m*/*z* (%): 471.6404 (100), calculated 471.6450 (100), corresponding to complex $[L+Zn]^{2+}$. ^{31}P NMR ($CDCl_3$, 500 MHz): 62.231 (s).

3.3.2. Synthesis of the complex ***2·Cu (ClO₄)₂***. $Cu(ClO_4)_2\cdot 6H_2O$ (0.38 g, 0.09 mmol); **2** (0.80 g, 0.09 mmol). Diethylether was allowed to diffuse into the filtrate to obtain the desired complex in 80% yield that was dried under vacuum. FTIR (KBr) (ν/cm^{-1}): 3449b, 2928m, 2972m, 1570s, 1509s, 1425m, 1354s, 1261m, 1076s. ESI-HRMS, *m*/*z* (%): calculated 471.1475 (100), found 471.1407 (100), corresponding to the complex $[L+Cu]^{2+}$.

3.3.3. Synthesis of the complex ***1****·Cu(ClO₄)₂*. $Cu(ClO_4)_2\cdot 6H_2O$ (0.038 g, 0.09 mmol); **1** (0.80 g, 0.11 mmol). Diethylether was allowed to diffuse into the filtrate to obtain the desired complex in 70% yield that was dried under vacuum. FTIR (KBr) (ν/cm^{-1}): 3448b, 2977m, 1720.81m, 1574s, 1511s, 1429m, 1380s, 1261m, 1190s, 1135s, 1076s. ESI-HRMS, *m*/*z* (%): calculated 365.6130 (100), found 365.2475 (100) corresponding to complex $[L+Cu]^{2+}$.

3.3.4. Synthesis of the complex ***3****·Cu(ClO₄)₂*. $Cu(ClO_4)_2\cdot 6H_2O$ (0.07 g, 0.18 mmol); **3** (0.10 g, 0.06 mmol). Yield: 0.076 g (73.0%). FTIR (KBr) (ν/cm^{-1}): 3448b, 2924s, 2854m, 1710.81m, 1655m, 1573s, 1510s, 1427m, 1378s, 1244m, 1134s, 1081s. ESI-HRMS, *m*/*z* (%): calculated 915.8541 (100), found 915.8317 (100) corresponding to complex $[L+Cu]^{2+}$.

4. Summary

In summary, we have demonstrated a simple approach for the design of fluorescence-based sensors. This methodology consists of assembly of phosphorus-supported coordinating platforms whose fluorescence properties are modulated by binding with Cu^{2+} as well as by the number of coordinating arms that the ligand possesses. We believe that this design is quite general and can be applied for selective detection of other type of metal ions also. We are currently studying these aspects.

Supporting information

CCDC 737014–737015 (for compounds **2** and **4**) contain the supplementary crystallographic data for this paper. These data can be obtained free of charge from The Cambridge Crystallographic Data Centre via www.ccdc.cam.ac.uk/data_request/cif.

Acknowledgements

We thank the Department of Science and Technology, India for financial support. V.C. is a Lalit Kapoor Chair Professor of Chemistry. V.C. is thankful for the Department of Science and Technology for a J.C. Bose fellowship. This work is also supported by the *Bioinorganic Chemistry Initiative*, DST, India.

References and notes

1. De Silva, A. P.; Gunaratne, H. Q. N.; Gunnlaugsson, T.; Huxley, A. J. M.; McCoy, C. P.; Rademacher, J. T.; Rice, T. E. *Chem. Rev.* **1997**, *97*, 1515.
2. Valeur, B.; Leray, I. *Coord. Chem. Rev.* **2000**, *205*, 3.
3. Fabbrizzi, L.; Poggi, A. *Chem. Soc. Rev.* **1995**, *24*, 197.
4. Ji, H.-F.; Brown, G. M.; Dabestani, R. *Chem. Commun.* **1999**, 609.
5. Ghosh, P.; Bharadwaj, P. K.; Mandal, S.; Ghosh, S. *J. Am. Chem. Soc.* **1996**, *118*, 1553.
6. Bolletta, F.; Costa, I.; Fabbrizzi, L.; Licchelli, M.; Montalti, M.; Pallavicini, P.; Prodi, L.; Zaccheroni, I. *J. Chem. Soc., Dalton Trans.* **1999**, 1381.
7. Sessler, J. L.; Davis, J. M. *Acc. Chem. Res.* **2001**, *34*, 989.
8. Goldsmith, C. R.; Lippard, S. J. *Inorg. Chem.* **2006**, *45*, 6474.
9. Wu, D.; Huang, W.; Duan, C.; Zhihua Lin, Z.; Meng, Q. *Inorg. Chem.* **2007**, *46*, 1538.
10. Yang, J. S.; Lin, C. S.; Hwang, C. Y. *Org. Lett.* **2001**, *3*, 889.
11. Hennrich, G.; Walter, W.; Resch-Genger, U.; Sonnenschein, H. *Inorg. Chem.* **2001**, *40*, 641.
12. Zheng, Y.; Orbulescu, J.; Ji, X.; Andreopoulos, F. M.; Pham, S. M.; Leblanc, R. M. *J. Am. Chem. Soc.* **2003**, *125*, 2680.
13. Kim, S. K.; Lee, S. H.; Lee, J. Y.; Lee, J. Y.; Bartsch, R. A.; Kim, J. S. *J. Am. Chem. Soc.* **2004**, *126*, 16499.

14. Sheng, R.; Wang, P.; Gao, Y.; Wu, Y.; Liu, W.; Ma, J.; Li, H.; Wu, S. *Org. Lett.* **2008**, *10*, 5015.
15. Kim, H. J.; Park, Y. S.; Yoon, S.; Kim, J. S. *Tetrahedron* **2008**, *64*, 1294.
16. Ramachandram, B.; Samanta, A. *Chem. Commun.* **1997**, 1037.
17. Ghosh, P.; Bharadwaj, P. K.; Roy, J.; Ghosh, S. *J. Am. Chem. Soc.* **1997**, *119*, 11903.
18. Ramachandram, B.; Samanta, A. *J. Phys. Chem. A* **1998**, *102*, 10579.
19. Kaur, S.; Kumar, S. *Chem. Commun.* **2002**, 2840.
20. Wu, Q.; Anslyn, E. V. *J. Am. Chem. Soc.* **2004**, *126*, 14682.
21. Wen, Z.-C.; Yang, R.; He, H.; Jiang, Y.-B. *Chem. Commun.* **2006**, 106.
22. Martinez, R.; Zapata, F.; Caballero, A.; Espinosa, A.; Tárraga, A.; Molina, P. *Org. Lett.* **2006**, *8*, 3235.
23. Martinez, R.; Espinosa, A.; Tárraga, A.; Molina, P. *Org. Lett.* **2005**, *7*, 5869.
24. Ravikumar, I.; Ahamed, B. N.; Ghosh, P. *Tetrahedron* **2007**, *63*, 12940.
25. Yang, L.; McRae, R.; Henary, M. M.; Patel, R.; Lai, B.; Vogt, S.; Christoph, J.; Fahrni, J. C. *PNAS* **2005**, *102*, 11179.
26. Rurack, K.; Kollmannsberger, M.; Resch-Genger, U.; Daub, J. *J. Am. Chem. Soc.* **2000**, *122*, 968.
27. Xu, Z.; Xiao, Y.; Qian, X.; Cui, J.; Cui, D. *Org. Lett.* **2005**, *7*, 889.
28. Royzen, M.; Dai, Z.; Canary, J. W. *J. Am. Chem. Soc.* **2005**, *127*, 1612.
29. Park, S. M.; Kim, M. H.; Choe, J.-I.; No, K. T.; Chang, S.-K. *J. Org. Chem.* **2007**, *72*, 3550.
30. Gitlin, J. D. *Gastroenterology* **2003**, *125*, 1868.
31. Mercer, J. F. B. *Trends Mol. Med.* **2001**, *7*, 64.
32. Multhaup, G.; Schlicksupp, A.; Hesse, L.; Beher, D.; Ruppert, T.; Masters, C. L.; Beyreuther, K. *Science* **1996**, *271*, 1406.
33. Waggoner, D. J.; Bartnikas, T. B.; Gitlin, J. D. *Neurobiol. Dis.* **1999**, *6*, 221.
34. Chandrasekhar, V.; Azhakar, R.; Andavan, G. T. S.; Krishnan, V.; Zacchini, S.; Bickley, J. F.; Steiner, A.; Butcher, R. J.; Kögerler, P. *Inorg. Chem.* **2003**, *42*, 5989.
35. Chandrasekhar, V.; Pandian, B. M.; Boomishankar, R.; Steiner, A.; Vittal, J. J.; Houri, A.; Clérac, R. *Inorg. Chem.* **2008**, *47*, 4918.
36. Chandrasekhar, V.; Pandey, M. D.; Bag, P.; Pandey, S. *Tetrahedron* **2009**, *65*, 4540.
37. Hirshberg, M.; Henrick, K.; Haire, L. L.; Nishi Vasisht, N.; Brune, M.; Corrie, T. E. J.; Webb, R. M. *Biochemistry* **1998**, *37*, 10381.
38. Jung, S. H.; Kwon, S. P.; Lee, W. J.; Hong, S. C.; Kim, W. J.; Yan, S.; Lee, Y. J.; Lee, H. J.; Joo, T.; Kim, S. J. *J. Am. Chem. Soc.* **2009**, *131*, 2008.
39. Ray, D.; Bharadwaj, K. P. *Inorg. Chem.* **2008**, *47*, 2252.
40. Wu, J.-S.; Liu, W.-M.; Zhuang, X.-Q.; Wang, F.; Wang, P.-F.; Tao, S.-L.; Zhang, X.-H.; Wu, S.-K.; Lee, S.-T. *Org. Lett.* **2007**, *9*, 33.
41. Lin, W.; Yuan, L.; Cao, Z.; Feng, Y.; Long, L. *Chem.—Eur. J.* **2009**, *15*, 5096.
42. Vilkov, L. V.; Sadova, N. I.; Zilberg, I. Y. *Zh. Strukt. Khim.* **1967**, *8*, 528.
43. Wingerter, S.; Pfeiffer, M.; Murso, A.; Lustig, C.; Stey, T.; Chandrasekhar, V.; Stalke, D. *J. Am. Chem. Soc.* **2001**, *123*, 1381.
44. Bag, B.; Bharadwaj, P. K. *J. Phys. Chem. B* **2005**, *109*, 4377.
45. Connors, K. A. *Binding Constants: The Measurement of Molecular Complex Stability*; John Wiley & Sons: New York, NY, 1987.
46. Sheldrick, G. M. *SHELXTL-97: A Program for Crystal Structure Refinement* (Release 97-2); University of Gottingen: Gottingen, Germany, 1997.
47. Paeker, C. A.; Ress, W. T. *Analyst* **1960**, *85*, 587.
48. Gabe, T.; Urano, Y.; Kikuchi, K.; Kojima, H.; Ngano, T. *J. Am. Chem. Soc.* **2004**, *126*, 3357.
49. Fery-Forgues, S.; Le Bries, M.-T.; Guetté, J.-P.; Valeur, B. *J. Phys. Chem.* **1988**, *92*, 6233.
50. Valeur, B. *Molecular Fluorescence Principles and Applications*; Wiley-VCH GmbH: New York, NY, 2001; p 341.
51. (a) Chandrasekhar, V.; Thangavelu, G.; Andavan, S.; Nagendran, S.; Krishnan, V.; Azhakar, R.; Butcher, J. R. *Organometallics* **2003**, *22*, 976; (b) Majoral, J.-P.; Kramer, R.; Navech, J.; Mathis, F. *Tetrahedron* **1976**, *32*, 2633.